

DOI: 10.1070/QEL16107

Study of the dielectric function of aqueous solutions of glucose and albumin by THz time-domain spectroscopy

M.M. Nazarov, O.P. Cherkasova, A.P. Shkurinov

Abstract. **We report a study of aqueous solutions of glucose and bovine serum albumin using THz time-domain spectroscopy. To describe the permittivity of the solutions of these substances, we use a simplified model being applicable in the frequency range of 0.05–2.7 THz. On the assumption that most of the water molecules become bound at high concentrations of glucose and protein in the solution, the changes in water characteristics are investigated. To improve the reliability of the results, the measurements are performed by two independent methods: the method of attenuated total internal reflection and the transmission method. Combination of the results obtained by these two methods allows expanding the spectral range towards lower frequencies.**

Keywords: *THz radiation, THz time-domain spectroscopy, attenuated total internal reflection, water, glucose, bovine serum albumin, solutions, dielectric function, Debye model.*

1. Introduction

Determination of concentrations of sugars and proteins in blood and tissues is important for medical and biological applications. It is known that the terahertz (THz) signal is changed in *in vivo* studies of THz radiation reflection from human or animal skin having a high glucose concentration in blood [1]. The main component of tissues and fluids in a body is water. The THz and sub-THz frequency bands can be used for the diagnosis of relative changes in the concentration and properties of water, since these frequencies correspond to the relaxation times of water molecules [2]. The state of the water itself, which is prevailing in these samples [3], represents a characteristic that is measured using THz spectroscopy. Changes in proportions of free and bound water, changes in relaxation times for each of these states of water – they are all manifested in the THz frequency range. Unfortunately, THz time-domain spectroscopy usually captures not the centre of a low-frequency 'peak' of water absorption (in the region near 0.02 THz), but its high-frequency 'tail', starting from the frequency of 0.1 THz (Fig. 1). Nevertheless, THz time-domain spectroscopy has become an established method which complements the existing methods of diagnostics of biological tissues and solutions. However, there is no consensus as to how to interpret the THz signal contrast in scanning the skin *in vivo* and how to predict the changes in the THz response of solutions.

M.M. Nazarov Institute of Laser and Information Technologies, Russian Academy of Sciences, Svyatoozerskaya ul. 1, 140700 Shatura, Moscow region, Russia; e-mail: nazarovmax@mail.ru;
O.P. Cherkasova Institute of Laser Physics, Siberian Branch, Russian Academy of Sciences, prosp. Akad. Lavrent'eva, 13/3, 630090 Novosibirsk, Russia; e-mail: o.p.cherkasova@gmail.com;
A.P. Shkurinov Faculty of Physics and the International Laser Centre, M.V. Lomonosov Moscow State University, Vorob'evy Gory 1, 119991 Moscow, Russia; Institute on Laser and Information Technologies, Russian Academy of Sciences, Svyatoozerskaya ul. 1, 140700 Shatura, Moscow region, Russia; e-mail: ashkurinov@gmail.com

Received 21 April 2016
Kvantovaya Elektronika **46** (6) 488–495 (2016)
Translated by M.A. Monastyrskiy

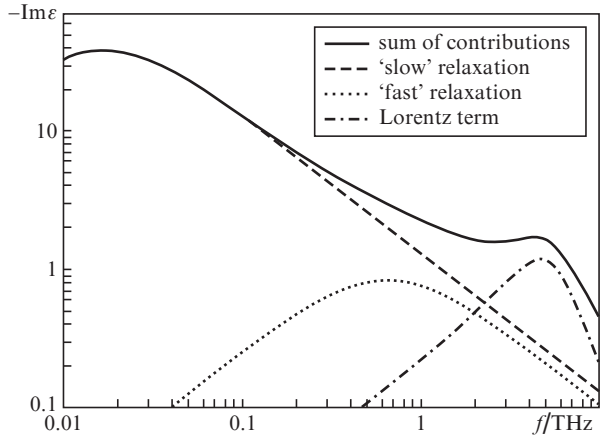

Figure 1. Spectra of the imaginary part of the permittivity $\mathrm{Im}\,\varepsilon(f)$ of water in the THz frequency range for a 'two-component' relaxation model.

Originally, the spectral response of a substance is given by its complex permittivity $\varepsilon(\omega)$. In the case of a homogeneous smooth object, absorption, refraction and reflection are uniquely determined by $\varepsilon(\omega)$. Historically, theory of the permittivity of water and water solutions has gained a greatest momentum in its development in the frame of dielectric spectroscopy when describing the changes observed in the experimental spectra of dielectrics [2, 4].

The relaxation processes in dielectrics, in the frequency range from kilohertz to gigahertz, can be divided into four types: α-, β-, γ- and δ-relaxations [2, 4, 5]. Each of these processes corresponds to its own wide frequency maximum which overlaps with neighbouring peaks and describes a specific relaxation process. For example, the α-relaxation describes the dielectric losses in glass-like dielectrics, and its relaxation times are equal to a few nanoseconds [2]. The γ-relaxation dominates for water, and its characteristic time amounts to tens of picoseconds (Fig. 1) [5, 6]. The external electromagnetic field sets the orientation of dipoles of water molecules. Under the impact of heat and entropy, molecules undergo a

rotational diffusion, so that a prominence of this orientation gradually disappears during the characteristic relaxation time τ. The water molecule possesses a specific structure which allows the formation of up to four hydrogen bonds with neighbouring molecules. The result is a three-dimensional structure of water molecules linked by hydrogen bonds [2, 7]. Namely this process of breaking the hydrogen bonds between water molecules with their subsequent reorientation constitutes the molecular basis of the γ-relaxation; in this case, τ represents the time required for release of water molecules from the network of hydrogen bonds [2, 8]. P. Debay proposed to describe the reaction of water to an external electric field by means of the complex permittivity in the form

$$\varepsilon(\omega) = \varepsilon'(\omega) - \mathrm{i}\varepsilon''(\omega) = \varepsilon_\infty + [\varepsilon(0) - \varepsilon_\infty]/(1 + \mathrm{i}\omega\tau), \qquad (1)$$

where $\omega = 2\pi f$ is the frequency of the external electric field; and ε_∞ and $\varepsilon(0)$ are the permittivities of water at the maximum and zero frequencies of the external field.

A number of authors have subsequently shown that in water, along with molecules bound by hydrogen bonds, there exist a small number of molecules that are not bound by any hydrogen bonds [8–10]. This state of water is described by the second term in the expression for the complex permittivity (1). The relaxation times of 'free' water molecules are more than by order of magnitude faster than those of the 'bound' molecules, that is why the second term has been called the fast Debye term (Fig. 1) [11, 12]. A two-component Debye model is traditionally used to describe the data obtained by means of THz time-domain spectroscopy [13–15].

With increasing the accuracy of measurements, it was found that even the two-component Debye formula does not always describe correctly the experimental data. Some modifications of expression (1), which take into account the deviations from the Debye dielectric spectrum of the solution [2], have been obtained for the sub-THz frequency range. In particular, in the frame of the Cole–Cole model, a formula containing the term $\mathrm{i}\omega\tau$ raised to a power lesser than unity has been proposed, which takes into account symmetrical broadening of the permittivity spectrum, which is observed in dissolving sugars and proteins in water [6, 16].

The most general formula that is currently used for analysing the dielectric response of polar solutions (in microwave and THz frequency range), is as follows:

$$\varepsilon(\omega) = \varepsilon_\infty + \frac{\Delta\varepsilon_1}{[1 + (\mathrm{i}\omega\tau_1)^\alpha]^\gamma} + \frac{\Delta\varepsilon_2}{1 + \mathrm{i}\omega\tau_2} + \frac{A_1}{\omega_{01}^2 - \omega^2 + \mathrm{i}\gamma_{01}\omega} + \frac{\mathrm{i}\sigma}{\omega\varepsilon_0} + \ldots, \qquad (2)$$

where the sum of amplitudes of all the terms must be equal to the statistical susceptibility

$$\varepsilon_s = \varepsilon_\infty + \Delta\varepsilon_1 + \Delta\varepsilon_2 + \frac{A_1}{\omega_{01}^2} + \ldots, \qquad (3)$$

where τ_1 and τ_2 are the relaxation times for the first (the main 'slow' γ-relaxation process) and second ('fast') Debye terms; $\Delta\varepsilon_i$ are the contributions to the permittivity of the first ($\Delta\varepsilon_1$) and second ($\Delta\varepsilon_2$) Debye terms; A_1 is amplitude; ω_{01} is frequency; γ_{01} is the Lorentz term linewidth; σ is static conductivity; and ε_0 is the dielectric constant. The values ε_s, $\Delta\varepsilon_1$ and τ_1 are exactly known from the dielectric spectroscopy data [2].

In this model (Fig. 1), about five variable parameters are distinguished; incorrect specification of one of them leads to erroneous values of the others, which is manifested in a noticeable divergence of the published data on Debye parameters of the THz response even for distilled water [11–14, 16–19] (Table 1).

The terms with higher frequencies are non-essential for the frequencies lesser than 5 THz. A model of the single Debye term (1) is more often used in the microwave and gigahertz (GHz) ranges; in this case, $\Delta\varepsilon_1 = \varepsilon_s - \varepsilon_\infty$, $\Delta\varepsilon_2 = 0$ and $A_1 = 0$. In the case of distilled water, the degrees of α and γ are equal to unity, while the conductivity $\sigma = 0$. When the dissolved substances appear in water, the degree of α becomes less than unity (the Cole–Cole model) [16], and the salt solutions (including the buffer) also acquire the conductivity σ [12, 20]. There is another new broadband measurement method in this frequency range, based on the optical Kerr effect [21, 22]. This method can be employed to simultaneously measure the parameters of the two above-mentioned relaxation processes, but the resulting values of τ_2 turn out overestimated compared with data obtained by means of THz time-domain spectroscopy.

Even for pure water, the multi-parametric model (2), (3) is not accurate and applicable in a wide frequency range. In particular, there are doubts whether the second fast Debye term proportional to ε_2 has a physical meaning and whether the relevant effect can be described by such a separate term. Perhaps this term does not describe an independent process and is associated with broadening of the wing of the γ-relaxation, which, with at least the same accuracy, can be described using a fractional degree of an additional term introduced into the denominator of the single slow Debye

Table 1. Parameters of the dielectric function of water.

f/THz	ε_s	ε_∞	$\Delta\varepsilon_1$	τ_1/ps	$\Delta\varepsilon_2$	τ_2/fs	A_1/ω_{01}^2	ω_{01}/THz	γ_{01}/THz	T/°C	Method	References
0.1–2.7	78.5	2.5±0.1	75±6	9.5±0.8	1.47±0.05	230±30	1.14	5.3	5.35	22	ATR	Present
0.08–1.1	77.5	2.4±0.02	72±2	9.5±0.3	2.0±0.04	300±30	1.12	5.3	5.35	22	THz-TDS	work
0.25–4.0	77.8	2.39	72.02	7.93	2.1	260	1.27	5.22	5.68	27	ATR	[16]
0.2–2.5	78.3	2.68	72.30	8.34	2.12	360	1.13	5.01	7.06	25	ATR	[19]
0.2–3.5	79.9	2.50	74.90	9.43	1.67	248	1.12	5.3	5.35	20	ATR	[17]
0.1–1.0	78.8	5.30	73.98	8.50	1.32	124	0	–	–	20	THz-TDS	[13, 14]
0.18–2.42 4.54–6.06	78.4	–	–	8.25	1.4±0.1	310±60	1.57	–	–	25	FTIR THz-TDS	[12]
1.5–6.67		2.20	71.49	8.31	2.80; 1.6	1.0; 0.10	1.12	5.26	4.34	25	FTIR	[11]
3×10^{-5}–0.1	78.4±0.1 80.2±0.1	5.2±0.1 5.6±0.1	73.16 74.60	8.27±0.2 9.36±0.5	0	–	0	–	–	25 20	DS	[18]

Notes: ATR is attenuated total internal reflection; THz-TDS is THz time-domain spectroscopy; DS is dielectric spectroscopy; FTIR is Fourier transform infrared spectroscopy.

term [2]. In addition, we do not know of any process/solution for which the contribution of this fast Debye term would be dominating.

Without a universally accepted model of what is happening with the water itself in the THz frequency range, there is no use in analysing the spectra of aqueous solutions in terms of variation in many parameters of the model. In describing a real solution with a single varied parameter (for example, the concentration of dissolved substances), it does not make any sense to vary three to five parameters in the expression for dielectric function of the solution, as it is now accepted. The need to vary all the parameters is most likely an indication of physical imperfectness of the model.

In this paper, we, in the first place, systematise the known parameters of a water model and refine the range of reasonable values for each of them at room temperature. In our view, the reference parameters of each relaxation process should be taken from a corresponding frequency range. In particular, for the most significant slow Debye γ-process (frequency range of 1–100 GHz, centred at a frequency of 20 GHz) we use the relevant dielectric spectroscopy data [18]. Fast parameters of the Debye process are agreed with the data obtained by means of THz time-domain spectroscopy, while the data for the high-frequency Lorentz term are taken from the Fourier transform infrared spectroscopy results [16] and are not varied. Thus, we obtain a simple model and relevant parameters which accurately enough describe both our experimental results and the data published by other authors for water in the frequency range of 0.05–3.0 THz.

Next we use parameters of a well-studied D-glucose solution in water, which are known both in GHz [23] and THz [16] range. The novelty of our work consists in measuring the spectra of BSA and glucose solutions in the THz frequency range (by adding low frequencies), and in observation of the changes over time in a solution of the glucose and BSA mixture.

2. Description of the dielectric function of polar solutions in the THz range

The model parameters of form (2) have been investigated by many research groups [11–14, 16–19]. Their values for the most typical cases are listed in Table 1. It can be seen that the scatter in each parameter is much greater than the approximation accuracy. It is also seen that the measured values of the same parameter are different for different frequency ranges and different measurement methods.

Thus, for approximating the dielectric function spectrum, certain constraints should be set on each parameter, proceeding from the data taken from the frequency range appropriate to each of the processes. In our case, to analyse the data in the range of 0.07–2.7 THz at room temperature (20–25 °C), we select the following parameter ranges, which do not contradict the literature data:

$$\varepsilon_\infty = 2.1–2.7,\ \Delta\varepsilon_1 = 72–75,\ \tau_1 = 8.3–9.5\ \text{ps},$$

$$\Delta\varepsilon = 1.4–2.1,\ \tau_2 = 130–360\ \text{fs},\ \varepsilon_s = 77–80.2.$$

Note that keeping the temperature constant is of importance [11, 17, 18, 21], because when the temperature changes from 20 °C to 25 °C, the time τ_1 is changed from 9.36 to 8.27 ps, which has a significant effect on the lower part of the THz spectrum. The character of evolution of the main parameters with increasing temperature by 1 °C relative to room temperature can be estimated, for example, with the use of the data published in [18] and presented in Table 1: τ_1 is changed by 2.4%, $\Delta\varepsilon_1$ – by 0.4%, and ε_∞ – by 1.5%.

For low (GHz and microwave) frequency ranges, the spectra of the dielectric function for aqueous solutions of sugars, protein and salt have been studied in detail by means of dielectric spectroscopy methods. It is known that the Cole–Cole model works well in this range [2, 20, 23]. With increasing solute concentration, the peak of the imaginary part of the dielectric function is broadened (in logarithmic scale); at the same time, its amplitude is reduced and the relaxation time τ of the process is increased. One of existing simplified explanations of the processes occurring in the solution of sugars when increasing the concentration is as follows [2]: the fraction of free water molecules decreases ($\Delta\varepsilon_1$ is reduced, τ_1 does not change), the fraction of bound water molecules [which has a different, greater τ_{1w}, such that the difference $1/\tau_1 - 1/\tau_{1w}$ between the corresponding frequencies is less than the spectral peak width in the dependence $\mathrm{Im}\,\varepsilon(\omega)$], while the sum of free and bound water contributions represents a peak of $\mathrm{Im}\,\varepsilon(\omega)$, which is moving to the left and downward. Some authors explain this by an increase in the effective value of τ_1, while the peak broadening is described by the degree reduction, α, in (2). At high concentrations ($C > 10$ mg mL^{-1}), the dependence of the parameters ($\Delta\varepsilon_1$, τ_1) on the concentration becomes slower, since the hydrate regions around each solute molecule start to intersect each other [16].

3. Setup and samples

The THz time-domain spectrometer [24, 25] and the calculation methods [26, 27] are described in detail in our previous works. The measurements of solution parameters were performed sequentially using two THz time-domain spectrometers: a 'low-frequency' spectrometer – in transmission configuration using a 500-μm-thick cuvette, and a 'high-frequency' spectrometer – in attenuated total internal reflection (ATR) configuration using a prism of high-resistance silicon with a right angle at the apex. In the low-frequency spectrometer, a pair of photoconductive antennas [25] at an average power of 10 mW (in the THz range) of a multi-dipole emitting antenna has been used. This efficient antenna allows one to illuminate a 0.5-mm-thick water sample by means of radiation at frequencies up to 1 THz (i.e. to measure a 1000-fold decrease in the THz field amplitude, herewith the power/energy is reduced by six orders!). For stable measurement of the extremely low frequencies (~0.07 THz), a long time sampling from 20 to 40 ps with respect to the THz pulse centre has been applied.

In the high-frequency spectrometer [24], the LT-GaAs surface and a 1-mm-thick ZnTe crystal have been used as a source and a receiver, respectively [25]. The average-power THz radiation of 100 nW was sufficient to measure the reflection spectrum in the range of 0.15–2.7 THz. Selection of a different source/receiver [25] allows measuring the reflection spectrum up to 3.5 THz, but to the detriment of frequencies lesser than 0.4 THz. This is not justified in the case of studying aqueous solutions, since the greatest changes occur in the low-frequency region. Such frequencies (0.07–0.2 THz) require a greater (2×2 cm) area of the sample located on a prism, a thick (1 mm) solution layer and a long (60 ps) time sampling.

To measure the real part of $\varepsilon(\omega)$ (actually, refraction) at low frequencies, more stable and accurate results are obtained when using a cuvette. However, for the frequencies greater

than 1 THz, it is better to use a prism because of a higher value of the high-frequency signal. Besides, use of a prism allows elimination of the error associated with the water layer thickness – a small change in this parameter introduces a noticeable error into the refraction data when working with a cuvette.

Characteristic spectra of the amplitude and phase of the reflection coefficient are shown in Fig. 2. Normalisation is performed relative to the spectrum of reflection from the prism with no solution.

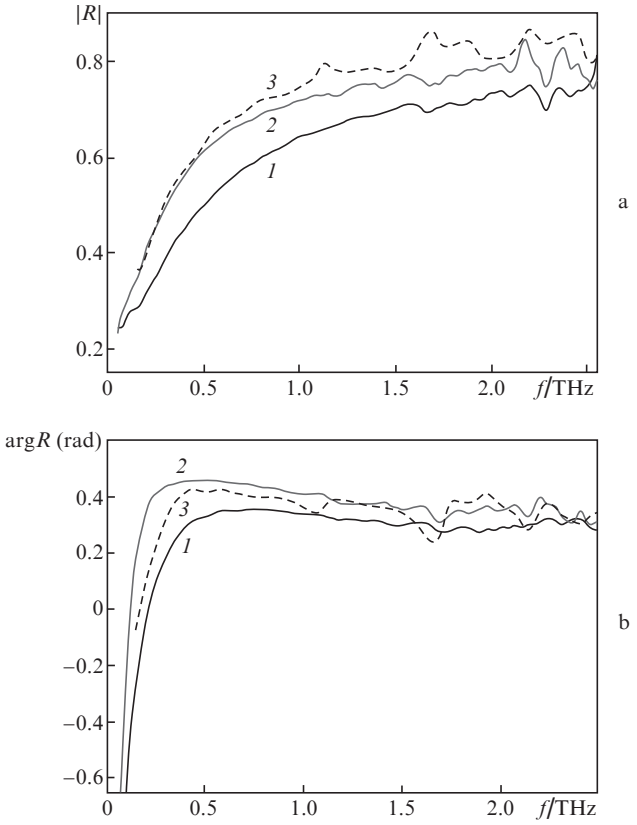

Figure 2. (a) Amplitude $|R|$ and (b) phase arg R spectra of the reflection coefficients for (*1*) water and aqueous solutions of (*2*) BSA and (*3*) glucose. The BSA concentration is 500 mg mL^{-1}, and the glucose concentration is 400 mg mL^{-1}.

Next the reflection and transmission spectra in complex form have been re-calculated according to the known Fresnel formulas [26, 27] into the spectrum of the complex permittivity, and combined for further analysis (Fig. 3).

We used solutions of the preparations of BSA and D-glucose (Sigma, USA) in double-distilled water. Dry preparations were weighed on an analytic balance and dissolved in water in order to obtain a desired concentration. Glucose solutions at a concentration of 270–840 mg mL^{-1} (1.5–4.7 M) and BSA solutions at a concentration of 30–500 mg mL^{-1} were studied. To carry out the glycation reaction, BSA was dissolved in phosphate buffer (50 mM, pH 7.4) at a concentration of 50 mg mL^{-1} and incubated with glucose (0.5 M) for 96 hours at a temperature of $T = 47$ °C. The solution volume for a single measurement in the ATR configuration constituted 800 μL, whilst in the transmission configuration, it was 400 μL.

In the data analysed below, each spectrum represents a result of averaging over five independent measurements. The

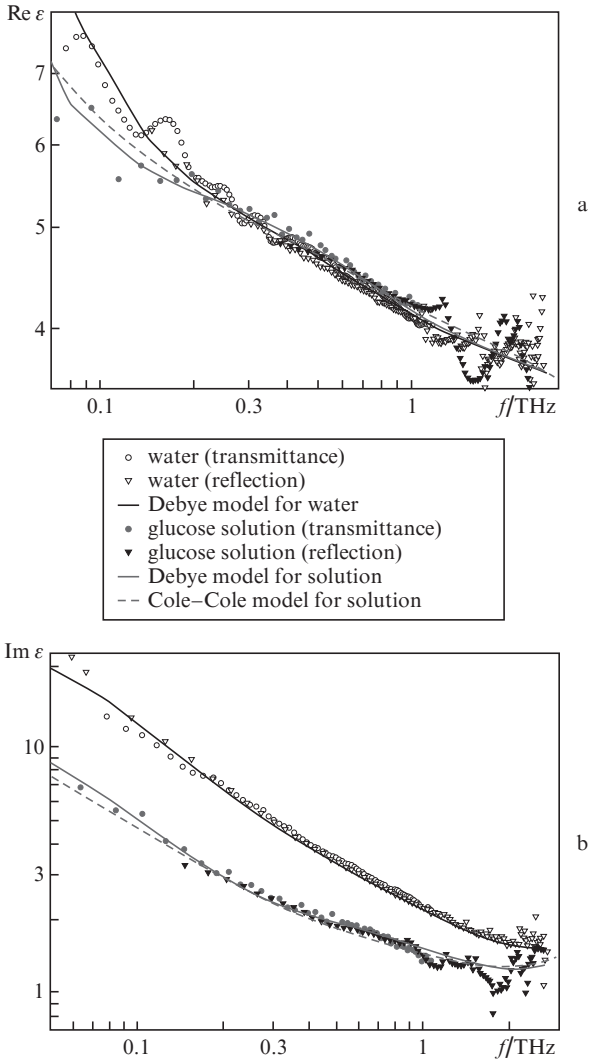

Figure 3. Spectra of (a) real and (b) imaginary parts of the dielectric function $\varepsilon(f)$ for a saturated aqueous solution of D-glucose and water at $T = 22$ °C. Points show combined experimental data on the transmittance and reflectance spectroscopy, solid curves are the Debye models, and the dashed curve is the Cole–Cole model.

repeatability of results at the frequencies of 0.5–1.0 THz re-calculated to $\varepsilon(\omega)$ constitutes about 3% and 1% for the real and imaginary parts, respectively. The instrumental errors associated with the accuracy of determination of the solution layer thickness in the cuvette and the angles of incidence in the prism, and also with finiteness of the time step, eventually lead to a total error of ~5%. This quantity represents namely the divergence of the values of $\varepsilon(\omega)$ converted from the data obtained by transmission and reflection methods at the frequencies of 0.5–1.5 THz. At the frequency spectrum edges (0.05–0.1 THz and 2–2.7 THz), the value of error $\varepsilon(\omega)$ repeatability amounts to 20% because of the low signal value (Fig. 3).

4. Results

As known from dielectric spectroscopy [20, 23], an increase in the concentration of glucose in water entails a decrease in the degree of α, an increase in the time τ_1, and a decrease in the amplitude $\Delta\varepsilon_1$ (the peak of the γ relaxation is broadened, shifted towards lower frequencies, and becomes lower). The authors of [16], who have investigated the solutions of glucose

Table 2. Dielectric function parameters at the frequencies of 0.04 and 0.15 THz for a solution of D-glucose in water and blood plasma (lower line).

C/mol L^{-1}	ε_s	ε_∞	$\Delta\varepsilon_1$	τ_1/ps	α	$\Delta\varepsilon_2$	τ_2/fs	T/°C	ε (0.04 THz)	ε (0.15 THz)	Method	References
0	78.5	2.5±0.1	75±6	9.5±0.8	1	1.5±0.05	230±30	22	17–i28	5.7–i8.9	ATR	Present work
1.5	60.0	2.49	53±2	9.5	1	1.6	230±20		13–i20	5.5–i6.3	THz-TDS	
4.7	34.3	2.5±0.02	29±0.3	9.5±0.3	1	1.7±0.03	230±20		9–i9	5.1–i3.3		
4.7	57.8	2.4±0.02	54±0.3	30±0.3	0.8	0,9±0.03	230±20		9–i9	5.7–i3.5		
0	77.8	2.39	72.02	7.93	1	2.1	260	27	20–i29	6.9–i9.9	ATR	[16]
1.5	55.8	2.39	50	7.93	1	2.1	220		16–i20	6.8–i7.3		
0	78.4	5.2	73.16	8.27	1	0	–	25	19–i29	6.4–i9.2	DS	[23]
1.5	74.8	2.85	72	13	0.87	0	–		14–i19	5.2–i7.2		
4.7	55.8	4.7	51.1	123	0.7	0	–		7–i3.8	5.6–i1.6		
0.9	70.6	5.6	65	12.6	0.9	0	–	Ambient			DS	[20]

by THz time-domain spectroscopy in the ATR configuration (in the frequency range being by the order of magnitude greater than in [20, 23]) give a different set of parameters (Table 2). As for our results, we have obtained a third set of parameters, different from those given in the literature. Thus, the values of the dielectric function at the frequencies for which both approaches are still applicable are in agreement with each other. The obtained experimental and model spectra of the dielectric function for the aqueous solution of glucose at a concentration of 4.7 M are shown in Fig. 3.

Of course, the real and imaginary parts of $\varepsilon(\omega)$ can be accurately approximated in the case of several varying parameters. However, we perform fitting simultaneously for both parts of $\varepsilon(\omega)$, which complicates obtaining an exact agreement between the model and experimental results in a wide frequency range. Using the parameters for a limiting glucose concentration found by the dielectric spectroscopy method [23] in the framework of the Cole–Cole model, $\alpha < 1$, we obtain a reasonable agreement with the results of a relevant THz experiment. On the other hand, when using the Debye model ($\alpha = 1$) we also obtain good agreement between the calculation and experimental results (Fig. 3). To this end, in the first approximation, we have multiplied the first Debye term's amplitude by the factor of 0.35. To ensure a more accurate approximation, we have selected the values of other parameters, which have been changed in this case less than by 20% compared to the case of water (Table 2).

It is noteworthy that, at the concentration of 4.7 M, the fast Debye term's amplitude has not virtually changed despite the fact that the volume fraction of glucose for this concentration constitutes 0.55, i.e. half the volume of water has been replaced by glucose, while the amplitude of the characteristic spectral water response in the region of 1 THz remained virtually the same. This contradiction requires further investigation. The importance of saturated solution is also that it should not contain free water; hence, the THz spectrum of such a solution is determined by a response of the water bound to glucose.

Within the framework of a more rigorous description, one should take into account the fact that part of the water volume is replaced by amorphous glucose having no spectral peculiarities in the THz range. Some authors propose a way to separate the contributions of remaining free water, solute, and bound water [16, 28]. In our rough model, a decrease in the volume fraction of water is taken into account by a decrease in $\Delta\varepsilon_1$, which is sufficient, since the contribution of this term exceeds the remaining contributions proportional to $\Delta\varepsilon_2$ and A_1 in the frequency range used. In the case of a water-insoluble additive (oil suspension), it has been experimentally shown in [13] that the relevant THz spectrum can be described by the same Debye parameters with allowance for their dependence on concentration. In particular, the $\Delta\varepsilon_1$ parameter is changed in [13] by 73%, τ_1 – by 2.3%, $\Delta\varepsilon_2$ – by 2.1%, τ_2 – by 0.1% and ε_∞ – by 1.3%. The dependence of parameters on the glucose concentration in blood plasma in the frame of the Cole–Cole model within the GHz range is given in [20].

Thus, in the case of the glucose solution, the calculation results for both models (the Cole–Cole model and the two-component Debye model) are equally consistent with the measurement results. We believe that, instead of complicating the models used for the analysis of experimental data, it is necessary to improve the accuracy and repeatability of experiments and to expand the spectral range of a measurement. Having demonstrated the performance of our methods for the case of the well-known solution (glucose), we move on to more complex objects, i.e., proteins.

As is known from dielectric spectroscopy, the bound water in wet BSA powders and other proteins has the main response at the frequencies of 10^7–10^{10} Hz, while the response at higher frequencies (including the γ-relaxation) is weak [2, 29]. In the case of dilute solutions of proteins, the THz range contains a high-frequency tail of the γ-relaxation spectrum (slow Debye process) which is described by the Cole–Cole model. With increasing protein concentration, a peak in the dependence of $\mathrm{Im}\,\varepsilon(\omega)$ is broadened ($\alpha < 1$), while the time τ_1 is slightly increased [30]. A more-faster-than-linear dependence on the volume fraction of protein, along with a decrease in the γ-relaxation amplitude of $\Delta\varepsilon_1$, may be considered to be associated with the changes in the structure of free water near the protein, which should change the shape of the $\varepsilon(\omega)$ spectrum at the low-frequency edge of the THz range [31].

The authors of [32] ascertain that the protein solution absorption at frequencies of 220–325 GHz becomes greater than that of water for the BSA concentrations lesser than 17 mg mL^{-1}, although it is less at higher concentrations as in most publications.

From the data on THz time-domain spectroscopy, it is known that, with increasing concentration of proteins, the absorption and refraction of their aqueous solutions are reduced stronger than in the case of displacing the solvent volume by the protein added to water [33, 34]. At the high-frequency edge (2–4 THz) of the THz range, the presence of protein (in particular, of BSA) in solution decreases the absorption value, though the dependence on concentration remains nonlinear [28, 31].

The obtained spectra of real and imaginary parts of the permittivity for an aqueous BSA solution are shown in Fig. 4. In this case, we have used an atypically large concentration of BSA (500 mg mL^{-1}) to ensure a stronger manifestation of the

change in the bound water response. One can see from Fig. 4 that such a simple action as a decrease in the first Debye term's amplitude well describes the change in imaginary part of the resulting permittivity $\varepsilon(\omega)$ of the solution, while for the real part of $\varepsilon(\omega)$ there is some discrepancy in the frequency range from 0.1 to 0.3 THz. This discrepancy at low frequencies has been observed for the protein solutions by other authors of Ref. [32].

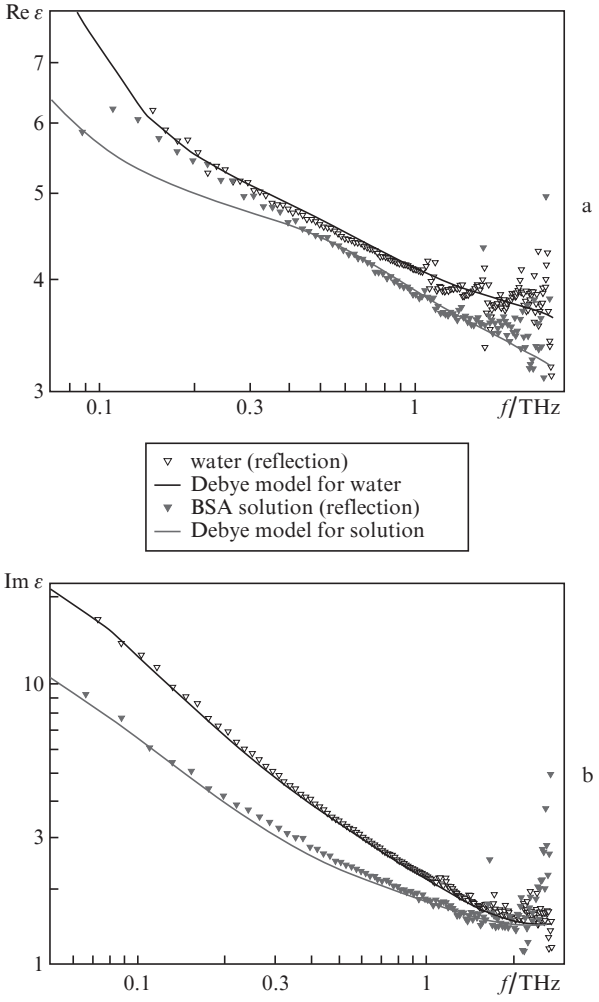

Figure 4. Spectra of (a) real and (b) imaginary parts of the dielectric function $\varepsilon(f)$ for an aqueous solution of BSA and water at $T = 22$ °C. Points show the experimental data on the reflectance spectroscopy, and solid curves are the Debye model.

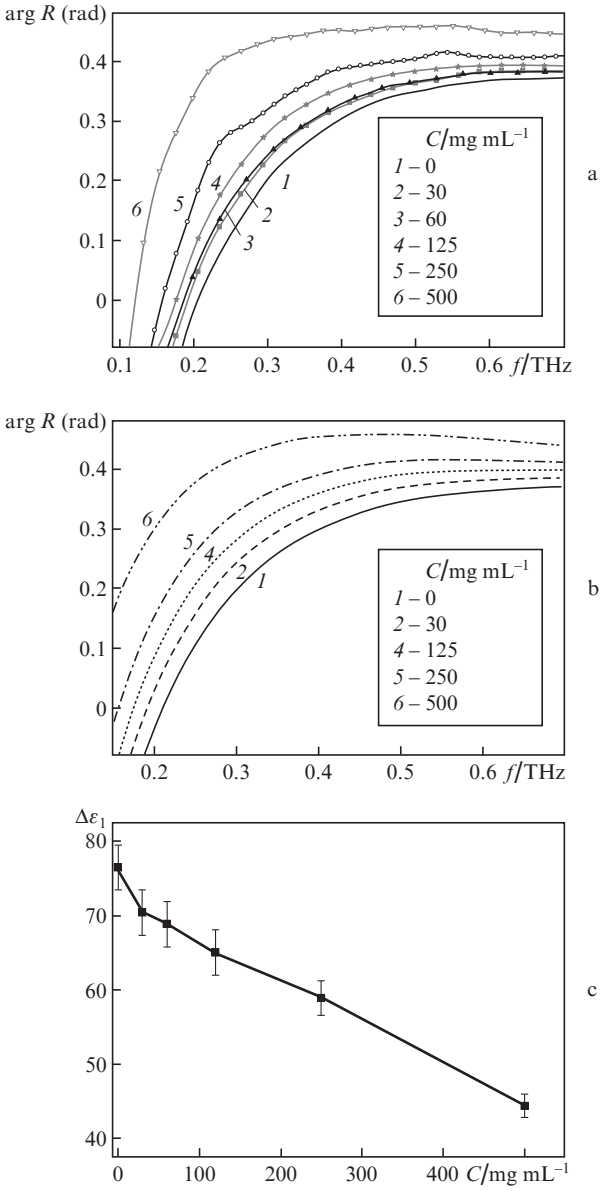

Figure 5. (a) Experimental and (b) model spectra of the phase arg R of the reflection coefficient of the BSA aqueous solution at various concentrations C (the experimental data are approximated by reducing the value of $\Delta\varepsilon_1$) and (c) the dependence of the parameter $\Delta\varepsilon_1$, found as a result of approximation, on the BSA concentration.

The most clear and stable solution spectrum changes occur when analysing the phase of the reflection coefficient at frequencies of 0.15–0.4 THz (Fig. 5a). Figure 5a clearly demonstrates a tendency to a change in the spectrum shape with increasing the BSA concentration. It is also seen that the results for a concentration of 30 mg mL^{-1} are still very different from the results at a zero concentration (i.e. for water). Similar data for the solution of one of the sugars (lactose) are given in [27].

At first glance it seems that the greatest changes during the BSA concentration growth are observed for the phase spectrum of the reflection coefficient at a frequency of 0.3 THz. However, this is due to the peculiarities of employing a prism in the ATR configuration – this frequency corresponds to the sharpest spectrum bend at an incidence angle of 57°. In fact, the biggest changes in the dielectric function occur at the lowest of the available frequencies. This can be seen in Figs 3 and 4.

The dependence of the parameter $\Delta\varepsilon_1$ on the protein concentration in solution has been constructed, based on the above-discussed model (2), (3) at fixed values of all terms apart from the first one (Fig. 5c). Actually, we cannot separate the effects of reducing $\Delta\varepsilon_1$ and increasing τ_1 if we proceed from the data corresponding to the frequencies greater than 0.1 THz. Both phenomena lead to the same change in the THz spectrum, since we have $\omega\tau_1 \gg 1$ in the denominator of the slow Debye term. We can only tell with certainty how the ratio $\Delta\varepsilon_1/\tau_1$ would change. We have postulated $\tau_1 = \text{const}$ in this case.

For a rough estimate of the changes in the THz spectrum of $\varepsilon(\omega)$ in the solution with increasing BSA concentration, it is possible to multiply $\Delta\varepsilon_1$ [or divide τ_1 (in ps)] by the value of $1 - 8\times10^{-4}C$ (where C is taken in mg mL^{-1}), although this estimate understates the impact of the protein presence at low concentrations.

Of practical interest is not a study of aqueous solutions of proteins or sugars separately, but a study of their mixtures. It is known that a high glucose level in human blood leads to glycation of proteins [35]. Mernea with co-authors [36] have recently published the results on the use of THz time-domain spectroscopy for studying the glycation dynamics of human serum albumin in the process of its incubation with glucose and fructose for 5–11 weeks. However, the change in the protein structure takes place at an early stage of glycation and leads to the formation of amadori products [37]. These products are accumulated in blood for several hours at high glucose concentrations [38]. In the present work, we used THz time-domain spectroscopy for studying the early stages of albumin glycation (0–96 hours). The BSA (50 mg mL^{-1}) was incubated in a phosphate buffer (50 mM, pH 7.4) in the presence of glucose (0.5 M) for 96 hours at $T = 47$ °C [39]. The formation of glycation products results in a change in BSA conformation and THz response of a modified protein solution.

Figure 6 shows the time dependence of the THz pulse amplitude after the beginning of incubation (in the original temporal representation), when the pulse passes through a solution layer with a thickness of 500 μm. Normalisation is performed with respect to the amplitude of the THz pulse that has passed through water. In terms of spectral representation, the dependence in Fig. 6 is a ratio of the transmittances of solution and water, averaged over the range of 0.1–1.0 THz. Since a solution is more transparent than a solvent, the relative transmittance is greater than unity. In the initial period of incubation, a considerable difference in transmittances of the solutions of pure BSA and its mixture with glucose is observed. Joining of glucose molecules to the amino acid residues of protein occurs during the BSA incubation with glucose [38]. This reduces the concentration of free glucose molecules in the solution in a mixture with BSA. As a result, a smaller proportion of water may be bound to glucose molecules, which causes an increase in the imaginary part of the permittivity, and, in turn, leads to a decrease in the transmittance of the initial mixture (Fig. 6).

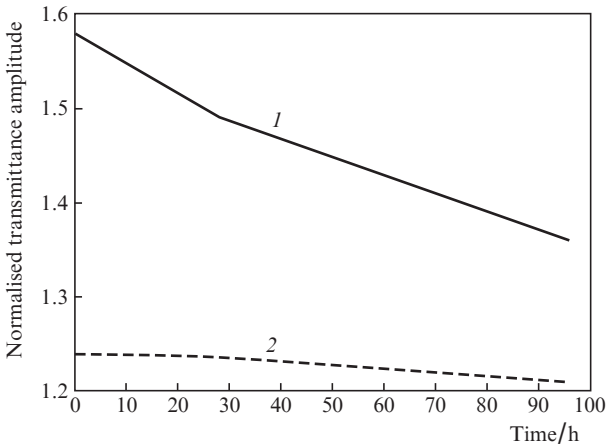

Figure 6. Time dependences of the normalised average transmittance amplitude after the beginning of the BSA incubation with glucose. Curve (*1*) shows a solution of the mixture of BSA and glucose, and curve (*2*) – a BSA control solution.

5. Conclusions

The dielectric function spectra of glucose and BSA aqueous solutions in the frequency range of 0.05–2.7 THz have been measured in detail. To derive a rough estimate of the causes of changes in the THz response of aqueous solutions, it was necessary to find out what is mostly varied in the dielectric function. We have found that the most significant is a decrease in $\Delta\varepsilon_1$ (or an increase in τ_1) with increasing solute concentrations. This variation alone is amply sufficient to describe with sufficient accuracy the observed changes in the THz response (both in reflection and transmission regimes) in the range of 0.05–2.7 THz. Proceeding from the model of the dielectric function with allowance for solute concentration, one can find out how the solution composition changes would manifest themselves in the radiation reflection from real biological objects (skin, blood, eye structures). We have shown that the best sensitivity to the changes in the composition of aqueous solutions is observed in the low-frequency range. Consequently, it is necessary to extend the spectral range towards low frequencies, preferably up to 20 GHz. The broadband measurements at the frequencies greater than 1 THz are unjustified, since in this frequency range the sensitivity to the changes in the composition of solutions and tissues is significantly lower, and no changes in spectral shape have been observed. We have identified which changes in the dependences obtained by THz time-domain spectroscopy are informative (change in low-frequency dispersion) and which of them are unreliable (general change in amplitude or shift in time).

In using the traditional model with the second fast Debye term, no significant changes in the assumed process parameters have been revealed even in the analysis of the spectra of saturated solutions, although it is in the investigated frequency range of 0.1–3.0 THz that this process should have been manifested to the greatest extent.

A nonstationary THz response has been observed during a few days in a mixture of solutions, which is probably due to a decrease in the hydration shell of glucose in the process of its attachment to the BSA.

Acknowledgements. The authors are grateful to Yu. Feldman for fruitful discussion of the results of this work.

References

1. Cherkasova O.P., Nazarov M.M., Shkurinov A.P. *Proc. IEEE 40th Int. Conf. on Infrared, Millimeter, and Terahertz Waves (IRMMW-THz)* (Hong Kong, 2015, F1E4). DOI:10.1109/IRMMW-THz.2015. 7327417).
2. *Dielectric Relaxation in Biological Systems: Physical Principles, Methods, and Applications*. Ed. by V. Raicu, Y. Feldman (Oxford: Oxford University Press, 2015).
3. Nazarov M., Shkurinov A., Tuchin V.V., Zhang X.-C. In: *Handbook of Photonics for Biomedical Science*. Ed. by V.V. Tuchin (Bosa Roca: CRC Press, Taylor & Francis Group, 2010) Ch. 23, p. 519.
4. Gusev Yu.A. *Osnovy dielektricheskoi spektroskopii* (Fundamentals of Dielectric Spectroscopy) (Kazan: Kazan State University, 2008) p. 112.
5. Sibik J., Zeitler J.A. *Adv. Drug Deliv. Rev.*, **100**, 147 (2016).

6. Wolf M., Gulich R., Lunkenheimer P., Loidl A. *Biochim. Biophys. Acta: Proteins Proteomics*, **1824** (5), 723 (2012).
7. Ben Ishai P., Tripathi S.R., Kawase K., et al. *Phys. Chem. Chem. Phys*., **17**, 15428 (2015).
8. Penkov N.V., Shvirst N.E., Yashin V.A., Fesenko E.E. *Biofiz.*, **58** (6), 933 (2013).
9. Walrafen G.E., Hokmabadi M.S., Yang W.-H. *J. Chem. Phys.*, **85**, 6964 (1986).
10. Robinson G.W., Cho C.H., Urquidi J. *J. Chem. Phys.*, **111**, 698 (1999).
11. Vij J.K., Simpson D.R.J., Panarina O.E. *J. Mol. Liq.*, **112**, 125 (2004).
12. Penkov N., Shvirst N., Yashin V., et al. *J. Phys. Chem. B*, **119** (39), 12664 (2015).
13. Reid C.B., Pickwell-MacPherson E., Laufer J.G., et al. *Phys. Med. Biol*., **55**, 1 (2010).
14. Fitzgerald A.J., Pickwell-MacPherson E., Wallace V.P. *PLoS One*, **9** (7), e99291 (2014).
15. Zaytsev K.I., Gavdush A.A., Chernomyrdin N.V., Yurchenko S.O. *IEEE Trans. Terahertz Sci. Technol.*, **5** (5), 817 (2015).
16. Shiraga K., Suzuki T., Kondo N., et al. *Carbohydr. Res.*, **406**, 46 (2015).
17. Yada H., Nagai M., Tanaka K. *Chem. Phys. Lett.*, **464**, 166 (2008).
18. Kaatze U. *J. Chem. Eng. Data*, **34**, 371 (1989).
19. Møller U., Cooke D.G., Tanaka K., Jepsen P.U. *J. Opt. Soc. Am. B*, **26** (9), A113 (2009).
20. Karacolak T., Moreland E.C., Topsakal E. *Microwave Opt. Technol. Lett.*, **55** (5), 1160 (2013).
21. Winkler K., Lindner J., Bürsing H., Vöhringer P. *J. Chem. Phys.*, **113**, 4674 (2000).
22. Turton D., Harwood T., Lapthorn A., et al. *Proc. SPIE Int. Soc. Opt. Eng.*, **8623**, 862303 (2013).
23. Fuchs K., Kaatze U. *J. Phys. Chem. B*, **105** (10), 2036 (2001).
24. Nazarov M.M., Shkurinov A.P., Kuleshov E.A., Tuchin V.V. *Kvantovaya Elektron.*, **38**, 647 (2008) [*Quantum Electron*., **38**, 647 (2008)].
25. Nazarov M.M., Shkurinov A.P., Angeluts A.A., Sapozhnikov D.A. *Izv. Vyssh. Uchebn. Zaved., Ser. Radiofiz.*, **52**, 595 (2009).
26. Cherkasova O.P., Nazarov M.M., Angeluts A.A., Shkurinov A.P. *Opt. Spektrosk*., **120** (1), 59 (2016).
27. Angeluts A.A., Balakin A.V., Evdokimov M.G., et al. *Kvantovaya Elektron.*, **44** (7), 614 (2014) [*Quantum Electron*., **44** (7), 614 (2014)].
28. Leitner D.M., Gruebele M., Havenith M. *HFSP J.*, **2** (6), 314 (2008).
29. Panagopoulou A., Kyritsis A., Shinyashiki N., Pissis P. *J. Phys. Chem. B*, **116**, 4593 (2012).
30. Basey-Fisher T.H., Hanham S.M., Andresen H., et al. *Appl. Phys. Lett.*, **99**, 233703 (2011).
31. Bye J.W., Meliga S., Ferachou D., et al. *J. Phys. Chem. A*, **118**, 83 (2014).
32. Sushko O., Dubrovka R., Donnan R.S. *J. Chem. Phys.*, **142**, 055101 (2015).
33. Vinh N.Q., Allen S.J., Plaxco K.W. *J. Am. Chem. Soc*., **133**, 8942 (2011).
34. Heyden M., Tobias D.J., Matyushov D.V. *J. Chem. Phys.*, **137**, 235103 (2012).
35. Friedlander M.A., Wu Y.C., Elgawish A., Monnier V.M. *J. Clin. Invest*., **97** (3), 728 (1996).
36. Mernea M., Ionescu A., Vasile I., et al. *Opt. Quantum Electron.*, **47** (4), 1 (2015).
37. Ansari N.A., Mir M.A.R., Habib S., et al. *Cell Biochem. Biophys.*, **70** (2), 857 (2014).
38. Chellan P., Nagaraj R.H. *J. Biol. Chem.*, **276** (6), 3895 (2001).
39. Lou H.X., Yuan H.Q., Yamazaki Y., et al. *Planta Med.*, **67**, 345 (2001).